Published in final edited form as:
Cancer Res. 2013 April 1; 73(7): 2117–2126. doi:10.1158/0008-5472.CAN-12-3957.

Autoimmune gastritis mediated by CD4+ T cells promotes the development of gastric cancer

Thanh-Long M. Nguyen[1], **Shradha S. Khurana**[2], **Clifford J. Bellone**[1], **Benjamin J. Capoccia**[2], **John E. Sagartz**[3], **Russell A. Kesman Jr.**[1], **Jason C. Mills**[2], and **Richard J. DiPaolo**[1]

[1]Department of Molecular Microbiology and Immunology, Saint Louis University School of Medicine, Saint Louis, Missouri

[2]Division of Gastroenterology, Washington University School of Medicine, St. Louis, Missouri

[3]Department of Comparative Medicine, Saint Louis University School of Medicine, Saint Louis, Missouri.

Abstract

Chronic inflammation is a major risk factor for cancer, including gastric cancers and other gastrointestinal cancers. For example, chronic inflammation caused by autoimmune gastritis (AIG) is associated with an increased risk of gastric polyps, gastric carcinoid tumors, and possibly adenocarcinomas. In this study, we characterized the progression of gastric cancer in a novel mouse model of AIG. In this model, disease was caused by CD4+ T cells expressing a transgenic T cell receptor specific for a peptide from the H+/K+ ATPase proton pump, a protein expressed by parietal cells in the stomach. AIG caused epithelial cell aberrations that mimicked most of those seen in progression of human gastric cancers, including chronic gastritis followed by oxyntic atrophy, mucous neck cell hyperplasia, spasmolytic polypeptide-expressing metaplasia (SPEM), dysplasia and ultimately gastric intraepithelial neoplasias (GIN). Our work provides the first direct evidence that AIG supports the development of gastric neoplasia, and provides a useful model to study how inflammation drives gastric cancer.

Keywords

gastric intraepithelial neoplasia; autoimmune gastritis; SPEM; chronic inflammation

Introduction

Autoimmune gastritis (AIG) is one of the most common autoimmune conditions in humans, and is caused when the adaptive immune system (T and B cells) targets self-antigens expressed by parietal cells and chief cells in the gastric mucosa. AIG may persist in an asymptomatic form for many years. A subset of individuals will eventually develop Pernicious Anemia (PA). PA is the major cause of vitamin B12 deficiency. AIG and PA have respective prevalence of 2 and 0.15–1% in the general population [1, 2], which is increased 3- to 5-fold in individuals with other, concomitant autoimmune diseases, such as type 1 diabetes [3, 4] and autoimmune thyroid disease [5, 6]. Gastric carcinoid tumors, evolving from enterochromaffine-like (ECL) cell hyper/dysplasia induced by

Address correspondence to: Dr. Richard DiPaolo Department of Molecular Microbiology and Immunology, Saint Louis University School of Medicine, Saint Louis, MO 63104 Phone: 314-977-8860, Fax: 314-977-8717 rdipaolo@slu.edu.

Disclosures: The authors disclose no conflicts

hypergastrinemia, develop in 4–9% of patients with AIG/PA [7-9]. Gastric carcinoid tumors are relatively benign lesions, metastasizing in less than 10% of cases [10]. Several studies have examined whether individuals with AIG/PA also have a higher risk of developing gastric adenocarcinomas, which is the second leading cause of cancer related deaths in the world. Two recent studies, one with 4.5 million retired male veterans in the USA and the other with included 9 million individuals from Sweden, reported that individuals with PA had an increased risk of developing not only gastrointestinal carcinoids, but also stomach adenocarcinomas, small intestinal adenocarcinomas, squamous cell carcinomas (SCC), and esophageal SCCs [11, 12].

Gastric cancer is the fourth most common cancer and the second most deadly malignant neoplasia in the world. A model, referred to as the Correa pathway, describes the development of gastric adenocarcinomas in humans from a histological perspective [13]. This model details the progression of gastric cancer through a series of pathological steps the epithelium undergoes starting with chronic inflammation (gastritis), followed by atrophy (especially loss of parietal cells), metaplasia, dysplasia, and eventually neoplasia. A better understanding of how inflammation induces gastric epithelial cell changes could provide potential therapeutic strategies for diagnosing and preventing gastric cancer [14]. To gain a better understanding of the progression of gastric cancer from a cellular and molecular perspective, numerous groups have developed animal models, mouse models in particular, to study gastric carcinogenesis. Such strategies have included chronic infection with *Helicobacter* [15], chemical depletion of parietal cells [16, 17], and several different lines of genetically modified mice. While these models have increased our understanding of the roles of infection, parietal cell loss, and genes involved in regulating epithelial cell biology, none have directly examined the role of chronic inflammation as the primary inducer of epithelial cell change, which would be useful for understanding the roles of cytokines and immune cells in promoting gastric cancer and for addressing the potential link between AIG and gastric cancer.

We investigated the potential link between AIG and gastric cancer using a T cell receptor (TCR) transgenic mouse model of AIG [18]. These transgenic $CD4^+$ T cells recognizes a peptide from the parietal cell specific antigen H^+/K^+ ATPase, which is also the major autoantigen targeted by the immune system in humans with AIG/PA [19]. All mice developed chronic gastritis that resulted from large numbers of $CD4^+$ T cells that infiltrated the gastric mucosa and produced large amounts of IFN-γ and smaller amounts of IL-17. Mice developed severe oxyntic atrophy and metaplasia by 2 to 4 months of age. At this stage of disease, mice also developed several molecular features associated with the progression of gastric cancer in humans, including spasmolytic polypeptide expressing metaplasia (SPEM), increased levels of mRNA for gastric cancer biomarkers (HE4, OLFM4, TFF2), and increased levels of phosphorylated STAT3 compared to non-transgenic control mice. Finally, by 12 months of age, all mice with AIG developed high grade dysplasia consistent with gastric intraepithelial neoplasia (GIN). In summary, we report a new mouse model demonstrating that inflammation associated with AIG induces many of the pathologic and molecule features of gastric carcinogenesis, including the development of severe dysplasia/GIN. These studies support a link between AIG and gastric cancer and highlight the importance of localized inflammation in the development of stomach cancer. This new, immune-system-induced model of gastric cancer will be useful for studying important host factors that influence inflammation induced adenocarcinomas.

Material and Methods

Mice

TxA23 TCR transgenic mice have been previously described, and have been bred >15 generations onto the BALB/c background [18]. The BALB/c control mice described in these experiments are TCR transgene negative littermates that were co-housed with the TxA23 TCR transgenic mice. All mice were maintained under specific pathogen-free conditions and cared for in our animal facility in accordance with institutional guidelines. Our colony tested negative by PCR for the following: Helicobacter bilis, Helicobacter hepaticus, Helicobacter rodentium, Helicobacter sp., Helicobacter trogontum, and Helicobacter typhlonius.

Histopathology

Stomachs were removed from mice, rinsed in saline, immersion fixed in 10% neutral-buffered formalin (Thermo Scientific), paraffin embedded, sectioned, and stained with hematoxylin and eosin. Pathology scores were assigned using methods modified from Rogers et. al. [20]. Slides were blinded and sections from individual mice were assigned scores between 0 (absent) and 4 (severe) to indicate the severity of inflammation, oxyntic atrophy, mucinous hyperplasia/metaplasia, and dysplasia. Scores were validated by an independent second pathologist blinded to experimental conditions.

Immunofluorescence

Stomachs were fixed for 20 minutes with methacarn (60% methanol, 30% chloroform and 10% glacial acetic acid (all from Fisher)), washed with 70% ethanol, embedded in paraffin and sectioned into 0.5μm thick sections. Slides were deparaffinized, rehydrated, stained, and imaged using methods modified from Ramsey et. al. [21]. The primary antibodies used for immunostaining were rabbit anti-human gastric intrinsic factor (gifts of Dr. David Alpers, Washington University), rabbit anti-Ki67 (Abcam), and mouse anti-Ecadherin (BD Bioscience). Secondary antibodies and GSII lectin (Molecular Probes) labeling were as described [21].

A gastric unit is defined as an invagination of the gastric mucosa that is lined by a single layer of columnar epithelium. Each gastric unit is lined by foveolar cells at the luminal end and zymogenic cells at the base. Ki67 staining was quantified by counting each Ki67+ nucleus per gastric unit for >50 units per mouse and classified into <10, 10-20 and >20 positive nuclei per unit. Percentages were calculated by dividing the number of gastric units in each category by total number of gastric units analyzed in that mouse stomach sample.

Immunohistochemistry

Tissue was deparaffinized and rehydrated. Endogenous peroxidase was blocked using a 0.3% H_2O_2 in methanol for 15 minutes. Antigen retrieval was done in a pressure cooker with Diva (Biocare: DV2004MX). Avidin/biotin kit (Biocare) was used to block endogenous biotin. The antibody pStat3 (D3A7) from Cell Signaling was diluted in Davinci (Biocare) and incubated over night at 4°C. The secondary antibody, biotinylated goat anti-rabbit and streptavidin-HRP from Jackson Labs were each applied for 1 hour at room temperature. Visualization was done with Biocare's Betaziod DAB and slides were counterstained in hematoxylin.

Immunoblot

A section from the stomach was homogenized with an electric pestle tissue homogenizer. Cells were then lysed in .5 ml of lysis buffer (20 mM Tris-HCl pH 7.5, 150 mM NaCl, 1 mM Na_2EDTA, 1 mM EGTA, 1% Triton, 2.5 mM sodium pyrophosphate, 1 mM beta-

glycerophosphate , 1 mM Na_3VO_4, 1 μg/ml leupeptin (Cell Signaling) and a protease inhibitor cocktail (Sigma)). Lysates were vortexed for 1 minute and sonicated for 15 seconds followed by centrifugation for 10 min at 4°C. Lysates were ran on a NuPAGE 4-12% BIS-TRIS gradient gel (Novex) and transferred to a nitrocellulose membrane. Membrane was blocked for 1 hour with 5% non-fat dairy milk. Primary antibodies (all from Cell Signaling) were stained for 1 hour (rabbit mAB-β-Actin-and rabbit mAB-STAT3) or overnight (rabbit mAB-Phospho-STAT 3) in 5% bovine serum albumin in 4°C. HRP-Linked secondary antibody (anti-rabbit IgG) was stained for 1 hours at room temperature in 5% non-fat dairy milk. Protein was detected by chemiluminescence using LumiGLO (Cell Signaling) on CL-XPosure X-Ray film (Fisher).

Flow cytometry

Cell surface staining was performed according to standard procedures using monoclonal antibodies against CD4, CD19, CD11b and Ly6G. Intracellular cytokine staining was performed using monoclonal antibodies against IFNγ and IL-17A. All antibodies were purchased from BD Pharmingen. All flow cytometry was performed on a BD LSRII or BD FACSCalibur and analyzed using FlowJo (TreeStar). For intracellular cytokine staining, cells were stimulated with PMA (Calbiochem) and Ionomycin (Calbiochem) for 4 hours at 37°C. Golgi-stop (BD Bioscience) was added after 1 hour. Cells were then washed, fixed in 4% formyl saline, washed, and permeabilized (0.5% BSA, 0.1% Triton, and 2mM EDTA in PBS) for 1 hr at room temperature. After washing, cells were incubated overnight with the anti-cytokine antibodies, washed and analyzed by flow cytometry.

Isolation of cells from the gastric lymph nodes and gastric mucosa

The method for isolating cells from the stomach tissue has been described previously [22, 23]. Briefly, the gastric lymph nodes (gLN) were removed from the stomachs, homogenized, and passed through a 40-μM pore nylon filter. Stomachs were opened with an incision from the antrum to the fundus, and rinsed in PBS to remove food. Cells were flushed from the gastric mucosa using a syringe with a 25 gauge needle. PBS containing 5% FCS and penicillin/streptomycin (Sigma) was repeatedly injected within the mucosa causing the tissue to swell and rupture. Single cell suspensions were collected, gently vortexed, and passed through a 40-μM nylon filter. Cells were counted, stained with antibodies, and analyzed by flow cytometry. To detect secreted cytokines, 1×10^6 cells were culture *in vitro* in 24 well plates containing 2 mL of supplemented RPMI. Supernatants from cell cultures were collected after 48 hours and cytokines and chemokines were measured using Milliplex (Millipore).

Quantitative Real Time PCR

Total RNA was prepared using the RNeasy Mini Kit system (Qiagen). The quantity and quality of RNA was determined using a NanoDrop 2000 spectrophotometer (Thermo Scientific) and 0.5 μg of the RNA was used to generate a first strand cDNA copy according to the manufacturer's instruction (High Capacity cDNA Reverse Transcription Kit, Applied Biosystems). Quantitative PCR was performed using TaqMan® Gene Expression Assays systems (Applied Biosystems). GAPDH served as an internal reference standard. PCR was ran on the 7500 Real-Time PCR System (Applied Biosystems).

Statistical Analysis

Data are expressed as means of individual determinations +/− standard error. Statistical analysis was performed using the Mann-Whitney Test (*P<.05; **P<.01; ***P<.001) using GraphPad Prism 5.

Results

Inflammation in TxA23 mice is characterized by CD4$^+$ T cells secreting IFN-γ and IL-17

Our first goal was to characterize the cell types and cytokines of TxA23 mice. Cells were isolated from the gastric mucosa and gastric lymph nodes of 2 month old mice and analyzed by flow cytometry. The majority (>85%) of the hematopoietic derived cells isolated were either CD4$^+$ T cells or CD19$^+$ B cells (Figure 1A). As expected, the majority of the CD4$^+$ T cells that infiltrated the stomach expressed the transgenic TCR (TCRVα2/TCRVβ2) specific for the H^+/K^+ ATPase peptide (Figure 1B). Macrophages (CD11b$^+$Ly6G$^-$) and neutrophils (CD11b$^+$Ly6G$^+$) and a subset of dendritic cells (CD11b+CD11c+, data not shown) comprised the rest of the cells found in the gastric mucosa (Figure 1C). Next, cells were re-stimulated and cytokine production by CD4$^+$ T cells was determined by intracellular cytokine staining. The majority of cytokine producing CD4$^+$ T cells isolated from the stomachs and gastric lymph node produced IFN-γ, and fewer produced IL-2, and IL-17. IL-4 secretion by CD4$^+$ T cells was not detected (Figure 1D). Finally, total cells isolated from the gastric lymph node were cultured immediately after isolation. The amounts of several cytokines secreted into the supernatants were determined after 48 hours. The most abundant cytokines secreted by cells were IFN-γ and IL-17 (Figure 1E). Lower levels of IL-6, IL-2, IL-10, and IL-4 were also detected. Thus the inflammatory cell infiltrate within the gastric mucosa consists primarily of a mixture of Th1 (IFN-γ$^+$) and Th17 (IL-17$^+$) CD4$^+$ T cells, and B cells. This type of inflammation is consistent with the types of inflammation described in humans infected with *H. Pylori* and with autoimmune gastritis [24, 25].

TxA23 progress through a series of pathological changes associated with the development of gastric cancer

In humans, the progression of intestinal-type gastric cancer is thought to evolve through a series of discrete steps known as the Correa pathway [13]. The first step in this pathway is inflammation (gastritis), then loss of parietal cells (oxyntic atrophy) and the development of mucinous metaplasia, followed by dysplasia and finally cancer. We examined the pathological features of gastric disease in TxA23 mice. At 2 months of age, TxA23 mice had moderate degrees of inflammation, oxyntic atrophy and mucosal hyperplasia/metaplasia, but little or no evidence of dysplasia (Figure 2A). By 4 months of age, inflammation, oxyntic atrophy, and mucosal hyperplasia/metaplasia were significantly more severe compared to 2 month old mice (Figure 2A). Lesions in the stomachs of 4 month old TxA23 mice comprised large areas in which parietal cells were either reduced in number or absent from the gastric units, and the remaining mucosa was dominated by large, hyperplastic mucus-containing cells that expanded to the bases of gastric units (Figure 2B-C). Four of the 19 mice had developed mild focal dysplasia (Figure 2D). For comparison, Figure 2E is representative of the normal pathology observed in 11 individual control mouse, which are transgene negative BALB/c mice that were co-housed with TxA23 littermates. Disease severity was similar in male and female mice at all ages. These data demonstrate that chronic inflammation resulting from autoimmune gastritis induced the development of preneoplastic lesions in the gastric mucosa of TxA23 mice with many pathological features in common with the Correa pathway.

Increased epithelial cell proliferation, phosphorylated STAT3, IL-6, and expression of gastric cancer-associated biomarkers in TxA23 mice

Next, we used immunofluorescence to compare the extent of gastric epithelial cell proliferation in 2 and 4 month old TxA23 mice compared to BALB/c control mice (Figure 3A-C). In wild type BALB/c mice, the number of proliferating (marked by Ki67$^+$ immunoreactivity) epithelial cells (marked by E-cadherin$^+$) per individual gastric unit was always less than 10. However, in TxA23 mice almost 70% of 2-month old gastric units had

10 or more proliferating cells, and by 4 months, more than 75% had more than 10 with about a third of those having 20 or more (Figure 3D).

Increased levels of the active (phosphorylated) signal transducer and activator of transcription 3 (pSTAT3) was involved in cellular transformation in numerous cancers of epithelial origin, including gastric cancer [26]. A recent study suggested that pSTAT3 is a significant prognostic factor in gastric cancer in humans [27]. To determine whether the level of pSTAT3 was increased in the stomachs of TxA23 mice, we performed western blots on gastric tissue lysates between age matched TxA23 and healthy BALB/c control mice. Compared to BALB/c mice, TxA23 mice expressed slightly higher levels of total STAT3 and a much higher level of pSTAT3 (Figure 4A). Immunohistochemical analysis revealed a large number of pSTAT3 positive epithelial cells present in the gastric mucosa of TxA23 mice, and nearly undetectable levels in gastric tissue from BALB/c controls (Figure 4B), in agreement with the results observed by Western blot.

Several members of the IL-6 cytokine family, including IL-6 and IL-11, activate STAT3 [28]. IL-6 and IL-11 have important roles in maintaining gastric homeostasis by regulating mucosal proliferation, inflammation, angiogenesis, and apoptosis [29, 30]. We performed quantitative real time PCR analysis using mRNA isolated from gastric tissue from 2 month old TxA23 and BALB/c mice to measure the relative levels of IL-6 and IL-11. The levels of IL-11 mRNA were equivalent between the two genotypes; however, the levels of IL-6 mRNA were ~40 fold higher in TxA23 mice compared to BALB/c mice (Figure 4C).

A number of genes have been described as biomarkers for precursor lesions like SPEM that are predisposing for gastric cancer. Some of these genes include Human Epididymis 4 (HE4) [16], Trefoil Factor 2 (TFF2) and Olfactomedin 4 (OLFM4) [31]. HE4 is absent in normal stomach and expressed in humans and mice with SPEM [16]. Increased levels of OLFM4, also known as GW112, have been observed in gastric cancers, including 58% of stage III/IV gastric cancers [31]. TFF2 is also known as spasmolytic polypeptide, and, by definition, increases when SPEM is present. We performed quantitative real time PCR analysis using mRNA isolated from sections taken from the body of the stomachs of TxA23 mice. All of the TxA23 mice expressed higher levels of HE4 and OLFM4, and a majority, 5 out of 7 mice, expressed higher levels of TFF2 compared to age-matched BALB/c control mice (Figure 4D). Together these data demonstrate that disease in TxA23 mice shares many of the molecular features of gastric cancer that have been reported in humans, including increased epithelial cell proliferation, increased levels of pSTAT3 protein, and higher levels of IL-6, HE4, OLFM4, and TFF2 mRNA.

SPEM is present in the gastric mucosa of TxA23 mice

Intestinal-type gastric cancer predominantly develops in the setting of oxyntic atrophy and mucous cell metaplasia [13]. Spasmolytic polypeptide-expressing metaplasia (SPEM), is a metaplasia in the gastric fundus resembling deep antral gland cells, and recent studies have indicated that SPEM may be directly linked to gastric neoplasia [25, 32]. We used immunohistochemistry to determine whether 4 month old TxA23 mice developed SPEM. A representative section from a TxA23 mouse is shown in figure 5A. In gastric units in which parietal cells have not yet been destroyed, chief cells are found at the base of the unit and are identified by staining with antibodies to gastric intrinsic factor (GIF). Of note, the antrum/pyloris of TxA23 mice were indistinguishable from BALB/c control mice. In the corpus region, neck cells are found above and identified by lectin GSII staining (Figure 5B). However, we also observed multiple gastric units in which the majority or all of the parietal cells had been lost (Figure 5B, C). In these parietal cell depleted units, there was an expansion of GSII-positive cells (mucous neck cell hyperplasia) and an emergence of cells expressing both neck cell specific and chief cell specific markers (GIF) in the base of the

units, whereas in regions with parietal cell preservation, the normal basal marker expression pattern was maintained (Figure 5D). Thus, GSII-positive GIF-positive cells in the base of gastric units that lack parietal cells also stained positive for TFF2 (data not shown), demonstrating13 that TxA23 mice developed regions of SPEM by 4 months of age.

TxA23 Mice Develop Gastric Intraepithelial Neoplasia (GIN)

In the next set of experiments we allowed a cohort of TxA23 mice to age, and performed histopathological evaluations to determine whether disease in TxA23 mice progressed beyond SPEM to dysplasia. Sections from stomachs of 4 and 12 month old mice were examined by a pathologist using a murine gastric histopathology scoring paradigm described previously [20] (Figure 6A). The analysis of mice at 4 months of age revealed that 15 of 19 had dysplasia scores of 0, and 4 of 19 mice had dysplasia scores of 1, indicating focal irregularly shaped gastric glands, including elongated, slit, trident, and back to back forms (Figure 6B). By 12 months of age, disease progressed to the point at which 7 of 8 mice developed severe dysplasia, indicated by scores of 3.5. In this scoring system a score of 3 is used to indicate severe loss of gland organization and columnar orientation, marked cell atypia, visible mitoses, gastric intraepithelial neoplasia (GIN), and 0.5 is added for carcinoma in situ or invasion without frank malignancy. We observed both focal and wide spread dysplasia, and most cases involved pseudoinvasion into the submucosa and/or serosa (Figure 6C-E). We also observed the formation of irregular glandular forms on the adventitial surface of the stomach, some of which contained papillary projections of atypical epithelium (Figure 6F). These data demonstrates that precancerous lesions observed in 4 month old TxA23 mice ultimately progressed to neoplastic disease.

Discussion

Although chronic atrophic gastritis is believed to be important in initiating gastric carcinogenesis, the precise role(s) of inflammation in the complex changes in gastric epithelial cells during the progression of gastric cancer are not understood. Furthermore, the relationship between AIG/PA and gastric cancer has been controversial and requires further investigation. In this study we describe a new mouse model demonstrating that autoimmune gastritis induces precancerous lesions similar to those that precede gastric cancer in humans. Mice with chronic inflammation caused by H^+/K^+ ATPase-specific $CD4^+$ T cells developed severe oxyntic atrophy coupled with metaplasia, including SPEM by 4 months of age. Similar to *H. pylori* infection and AIG in humans, inflammation in TxA23 mice contained $CD4^+$ T cells of the Th1 (IFN-γ^+) and Th17 (IL-17^+) phenotype [33, 34]. Consistent with the Correa pathway that describes the progression of gastric cancer in humans, TxA23 mice progressed through a series of stages that included inflammation, atrophic gastritis, mucous neck cell hyperplasia, SPEM, which over time progressed to dysplasia, and neoplasia. These data indicate that the TxA23 model system is unique in that it allows for the study of the development and regulation of gastric carcinogenesis in a setting where chronic inflammation, in the absence of infection, toxins, and drugs, is the primary upstream instigator. Our findings of carcinogenesis in our mouse model are consistent with reports that humans with AIG/PA are 3- to 6- times more likely to develop gastric adenocarcinoma and other cancers [35, 36]. It has been reported that a subset of individuals contain T cells and antibodies specific for H^+/K^+ ATPase after they are infected with *H. pylori* [37-40]. It is possible that individuals that develop autoimmune responses during *H. pylori* infection may remain at risk for gastric cancer even if they are treated for *H. pylori* infection. Studies have shown that the eradication of *H. pylori* reduces risk for subsequent gastric cancer by about 25% [40-42]. Strategies to reduce inflammation in addition to eradicating *H. pylori* may further reduce the risk of gastric cancer.

With the two recent studies reporting that individuals with Pernicious Anemia developed gastrointestinal cancers at a higher than expected rate, animal models that mimic AIG are likely to be useful for understanding the link between AIG and GI cancers. There is no doubt that infection with *H. pylori* is an important, prerequisite risk factor for gastric cancer; however, the vast majority of infected patients do not develop cancer. Therefore, it may be the types of chronic inflammation in the gastric mucosa that is triggered by *H. pylori* that are downstream adjuvants or causes of actual cancer. The TxA23 mouse model described here mimics the human disease and demonstrates the progression of AIG to the development of SPEM and eventually severe to dysplasia. Other genetically engineered mouse models have been useful for studying factors that influence the development of gastric cancer independently of *Helicobacter* infection. For example, mice expressing gastrin under the insulin promoter [43], mice deficient in: TFF1 [44], Smad4 [45], and Hip1r [46], and mice expressing a mutated form of the IL-6 family co-receptor gp130 [47] all develop forms of gastric metaplasia and some cases dysplasia. Our model specifically focuses on the immune response to H^+/K^+ ATPase and its role in promoting SPEM with progression to severe dysplasia. By inducing severe dysplasia in the absence of infection, this model will allow for a direct examination of the mechanisms whereby inflammation influences gastric epithelial cell biology. For example, when examining disease in cytokine knockout mice, using our model, we do not have to be concerned with the potential indirect effects of the importance of the cytokine in modulating *Helicobacter* infection itself. Our model will be also useful for evaluating the importance of immune cells, such as regulatory T cells and how they influence changes in gastric epithelial cells that are associated with the progression of gastric cancer. Finally, future studies using this model will address how various host factors, especially immune-related genes, influence the risk of developing gastric cancer.

Acknowledgments

We thank Joy Eslick and Sherri Koehm for assistance with flow cytometry and Jeremy Herzog for technical assistance. We also thank Anna Cline, Lauren Kintz, Erin Touchette, Kelly Neal, Frank Speck, and Dr. Cheri West for their assistance maintaining our mouse colonies. We also thank Dr. Deborah Rubin and Kymberli Carter from the Digestive Disease Research Core Center for assistance with immunohistochemistry, and the Washington University Digestive Disease Research Core Center for providing a Pilot & Feasibility grant.

Financial Support: RJD: (ACS:RSG-12-171-01-LIB, Digestive Diseases Research Core Center: NIH2P30 DK052574), JCM: (ACSDDC-115769, NIHDK094989-01; AGA Funderburg Research Scholar Award; Digestive Diseases Research Core Center: NIH2P30 DK052574-12); SSK: Siteman Cancer Pathways Award.

Grant Support RJD: (ACS:RSG-12-171-01-LIB, Digestive Diseases Research Core Center: NIH2P30 DK052574), JCM: (ACSDDC-115769, NIHDK094989-01; AGA Funderburg Research Scholar Award; Digestive Diseases Research Core Center: NIH2P30 DK052574-12); SSK: Siteman Cancer Pathways Award.

Abbreviations used

AIG	Autoimmune Gastritis
SPEM	spasmolytic polypeptide expressing metaplasia
GSII	Griffonia simplicifolia-II
GIF	gastric intrinsic factor
GIN	gastric intraepithelial neoplasia
TFF2	trefoil factor 2

References

1. Jacobson DL, et al. Epidemiology and estimated population burden of selected autoimmune diseases in the United States. Clin Immunol Immunopathol. 1997; 84(3):223–43. [PubMed: 9281381]
2. Carmel R. Prevalence of undiagnosed pernicious anemia in the elderly. Arch Intern Med. 1996; 156(10):1097–100. [PubMed: 8638997]
3. Riley WJ, et al. Predictive value of gastric parietal cell autoantibodies as a marker for gastric and hematologic abnormalities associated with insulin-dependent diabetes. Diabetes. 1982; 31(12): 1051–5. [PubMed: 7173496]
4. De Block CE, De Leeuw IH, Van Gaal LF. High prevalence of manifestations of gastric autoimmunity in parietal cell antibody-positive type 1 (insulin-dependent) diabetic patients. The Belgian Diabetes Registry. J Clin Endocrinol Metab. 1999; 84(11):4062–7. [PubMed: 10566650]
5. Centanni M, et al. Atrophic body gastritis in patients with autoimmune thyroid disease: an underdiagnosed association. Arch Intern Med. 1999; 159(15):1726–30. [PubMed: 10448775]
6. Irvine WJ, et al. Thyroid and gastric autoimmunity in patients with diabetes mellitus. Lancet. 1970; 2(7665):163–8. [PubMed: 4193564]
7. Kokkola A, et al. The risk of gastric carcinoma and carcinoid tumours in patients with pernicious anaemia. A prospective follow-up study. Scand J Gastroenterol. 1998; 33(1):88–92. [PubMed: 9489914]
8. Armbrecht U, et al. Development of gastric dysplasia in pernicious anaemia: a clinical and endoscopic follow up study of 80 patients. Gut. 1990; 31(10):1105–9. [PubMed: 2083855]
9. Borch K, Renvall H, Liedberg G. Gastric endocrine cell hyperplasia and carcinoid tumors in pernicious anemia. Gastroenterology. 1985; 88(3):638–48. [PubMed: 2578420]
10. Modlin IM, et al. Current status of gastrointestinal carcinoids. Gastroenterology. 2005; 128(6): 1717–51. [PubMed: 15887161]
11. Landgren AM, et al. Autoimmune disease and subsequent risk of developing alimentary tract cancers among 4.5 million US male veterans. Cancer. 2011; 117(6):1163–71. [PubMed: 21381009]
12. Hemminki K, et al. Effect of autoimmune diseases on mortality and survival in subsequent digestive tract cancers. Ann Oncol. 2012; 23(8):2179–84. [PubMed: 22228448]
13. Correa P. A human model of gastric carcinogenesis. Cancer Res. 1988; 48(13):3554–60. [PubMed: 3288329]
14. Goldenring JR, et al. Spasmolytic polypeptide-expressing metaplasia and intestinal metaplasia: time for reevaluation of metaplasias and the origins of gastric cancer. Gastroenterology. 2010; 138(7):2207–10. 2210, e1. [PubMed: 20450866]
15. Fox JG, et al. Hypertrophic gastropathy in Helicobacter felis-infected wild-type C57BL/6 mice and p53 hemizygous transgenic mice. Gastroenterology. 1996; 110(1):155–66. [PubMed: 8536852]
16. Nozaki K, et al. A molecular signature of gastric metaplasia arising in response to acute parietal cell loss. Gastroenterology. 2008; 134(2):511–22. [PubMed: 18242217]
17. Huh WJ, et al. Tamoxifen induces rapid, reversible atrophy, and metaplasia in mouse stomach. Gastroenterology. 2012; 142(1):21–24. e7. [PubMed: 22001866]
18. McHugh RS, et al. A T cell receptor transgenic model of severe, spontaneous organ-specific autoimmunity. Eur J Immunol. 2001; 31(7):2094–103. [PubMed: 11449363]
19. Callaghan JM, et al. Alpha and beta subunits of the gastric H+/K(+)-ATPase are concordantly targeted by parietal cell autoantibodies associated with autoimmune gastritis. Autoimmunity. 1993; 16(4):289–95. [PubMed: 7517707]
20. Rogers AB, et al. Helicobacter pylori but not high salt induces gastric intraepithelial neoplasia in B6129 mice. Cancer Res. 2005; 65(23):10709–15. [PubMed: 16322215]
21. Ramsey VG, et al. The maturation of mucus-secreting gastric epithelial progenitors into digestive-enzyme secreting zymogenic cells requires Mist1. Development. 2007; 134(1):211–22. [PubMed: 17164426]
22. Alderuccio F, et al. A novel method for isolating mononuclear cells from the stomachs of mice with experimental autoimmune gastritis. Autoimmunity. 1995; 21(3):215–21. [PubMed: 8822279]

23. DiPaolo RJ, et al. CD4+CD25+ T cells prevent the development of organ-specific autoimmune disease by inhibiting the differentiation of autoreactive effector T cells. J Immunol. 2005; 175(11): 7135–42. [PubMed: 16301616]
24. Shi Y, et al. Helicobacter pylori-induced Th17 responses modulate Th1 cell responses, benefit bacterial growth, and contribute to pathology in mice. J Immunol. 184(9):5121–9. [PubMed: 20351183]
25. Lopez-Diaz L, et al. Parietal cell hyperstimulation and autoimmune gastritis in cholera toxin transgenic mice. Am J Physiol Gastrointest Liver Physiol. 2006; 290(5):G970–9. [PubMed: 16399875]
26. Gong W, et al. Expression of activated signal transducer and activator of transcription 3 predicts expression of vascular endothelial growth factor in and angiogenic phenotype of human gastric cancer. Clin Cancer Res. 2005; 11(4):1386–93. [PubMed: 15746037]
27. Xiong H, et al. Constitutive activation of STAT3 is predictive of poor prognosis in human gastric cancer. J Mol Med (Berl). 2012; 90(9):1037–46. [PubMed: 22328012]
28. Silver JS, Hunter CA. gp130 at the nexus of inflammation, autoimmunity, and cancer. J Leukoc Biol. 88(6):1145–56. [PubMed: 20610800]
29. Jackson CB, et al. Augmented gp130-mediated cytokine signalling accompanies human gastric cancer progression. J Pathol. 2007; 213(2):140–51. [PubMed: 17724739]
30. Giraud AS, et al. Differentiation of the Gastric Mucosa IV. Role of trefoil peptides and IL-6 cytokine family signaling in gastric homeostasis. Am J Physiol Gastrointest Liver Physiol. 2007; 292(1):G1–5. [PubMed: 16935852]
31. Oue N, et al. Serum olfactomedin 4 (GW112, hGC-1) in combination with Reg IV is a highly sensitive biomarker for gastric cancer patients. Int J Cancer. 2009; 125(10):2383–92. [PubMed: 19670418]
32. Lennerz JK, et al. The transcription factor MIST1 is a novel human gastric chief cell marker whose expression is lost in metaplasia, dysplasia, and carcinoma. Am J Pathol. 2010; 177(3):1514–33. [PubMed: 20709804]
33. Mohammadi M, et al. Helicobacter-specific cell-mediated immune responses display a predominant Th1 phenotype and promote a delayed-type hypersensitivity response in the stomachs of mice. J Immunol. 1996; 156(12):4729–38. [PubMed: 8648119]
34. Smythies LE, et al. Helicobacter pylori-induced mucosal inflammation is Th1 mediated and exacerbated in IL-4, but not IFN-gamma, gene-deficient mice. J Immunol. 2000; 165(2):1022–9. [PubMed: 10878379]
35. Hsing AW, et al. Pernicious anemia and subsequent cancer. A population-based cohort study. Cancer. 1993; 71(3):745–50. [PubMed: 8431855]
36. Brinton LA, et al. Cancer risk following pernicious anaemia. Br J Cancer. 1989; 59(5):810–3. [PubMed: 2736218]
37. Ito M, et al. Role of anti-parietal cell antibody in Helicobacter pylori-associated atrophic gastritis: evaluation in a country of high prevalence of atrophic gastritis. Scand J Gastroenterol. 2002; 37(3): 287–93. [PubMed: 11916190]
38. Claeys D, et al. The gastric H+,K+-ATPase is a major autoantigen in chronic Helicobacter pylori gastritis with body mucosa atrophy. Gastroenterology. 1998; 115(2):340–7. [PubMed: 9679039]
39. Amedei A, et al. Molecular mimicry between Helicobacter pylori antigens and H+, K+ -- adenosine triphosphatase in human gastric autoimmunity. J Exp Med. 2003; 198(8):1147–56. [PubMed: 14568977]
40. D'Elios MM, et al. Molecular specificity and functional properties of autoreactive T-cell response in human gastric autoimmunity. Int Rev Immunol. 2005; 24(1-2):111–22. [PubMed: 15763992]
41. de Vries AC, Kuipers EJ, Rauws EA. Helicobacter pylori eradication and gastric cancer: when is the horse out of the barn? Am J Gastroenterol. 2009; 104(6):1342–5. [PubMed: 19491846]
42. Wong BC, et al. Helicobacter pylori eradication to prevent gastric cancer in a high-risk region of China: a randomized controlled trial. JAMA. 2004; 291(2):187–94. [PubMed: 14722144]
43. Wang TC, et al. Synergistic interaction between hypergastrinemia and Helicobacter infection in a mouse model of gastric cancer. Gastroenterology. 2000; 118(1):36–47. [PubMed: 10611152]

44. Lefebvre O, et al. Gastric mucosa abnormalities and tumorigenesis in mice lacking the pS2 trefoil protein. Science. 1996; 274(5285):259–62. [PubMed: 8824193]

45. Xu X, et al. Haploid loss of the tumor suppressor Smad4/Dpc4 initiates gastric polyposis and cancer in mice. Oncogene. 2000; 19(15):1868–74. [PubMed: 10773876]

46. Jain RN, et al. Hip1r is expressed in gastric parietal cells and is required for tubulovesicle formation and cell survival in mice. J Clin Invest. 2008; 118(7):2459–70. [PubMed: 18535670]

47. Judd LM, et al. Gastric cancer development in mice lacking the SHP2 binding site on the IL-6 family co-receptor gp130. Gastroenterology. 2004; 126(1):196–207. [PubMed: 14699500]

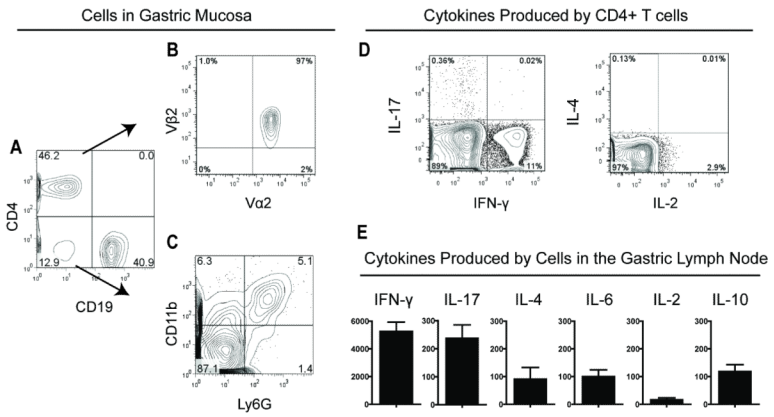

Figure 1. Inflammation in TxA23 mice

Representative Flow Cytometry plots of cell types and cytokines from a TxA23 mice (N=21). (**A**) Flow cytometry was used to identify T cells ($CD4^+$) and B Cells ($CD19^+$). (**B**)The majority of $CD4^+$ gated T cells express the transgenic TCR (TCRVα2/TCRVβ2) that recognizes a peptide from H^+/K^+ ATPase. (**C**) Macrophages ($CD11b^+Ly6G^-$) and neutrophils ($CD11b^+Ly6G^+$) make up a large proportion of the remaining cells. (**D**) Intracellular cytokine staining showing IL-17, IFN-y, IL-2 and IL-4 production by $CD4^+$ T cells combined from the gastric mucosa and lymph node. (**E**) Cytokines secreted by cells isolated from the gastric lymph nodes of TxA23 mice were measured by bead-based ELISA. Data are the mean +/− standard error of seven mice from three independent experiments.

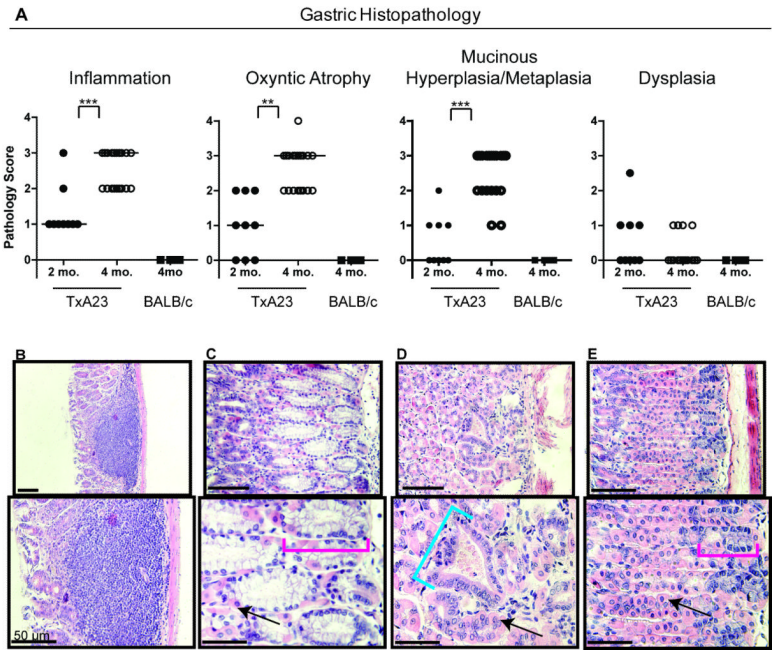

Figure 2. Preneoplastic lesions in TxA23 mice

(**A**) Pathology scores of stomach sections from 2 month old (N=9) and 4 month old TxA23 mice (N=19). (**B-D**) Representative images of pathology observed in TxA23 mice illustrating (**B**) inflammation, oxyntic atrophy, and mucosal hyperplasia. (**C**) Extensive parietal cell loss accompanied by moderate levels of mucinous metaplasia (red bracket). (**D**) Focal regions of mild dysplasia (blue bracket). (**E**) Normal morphology in a BALB/c control mouse with healthy parietal cells and basal non-metaplastic zymogenic chief cells at base of unit (red bracket denotes base region). Arrows point to healthy parietal cells. Statistics were performed using the Mann-Whitney U Test (*$** p < 0.01$, $*** p < 0.001$).

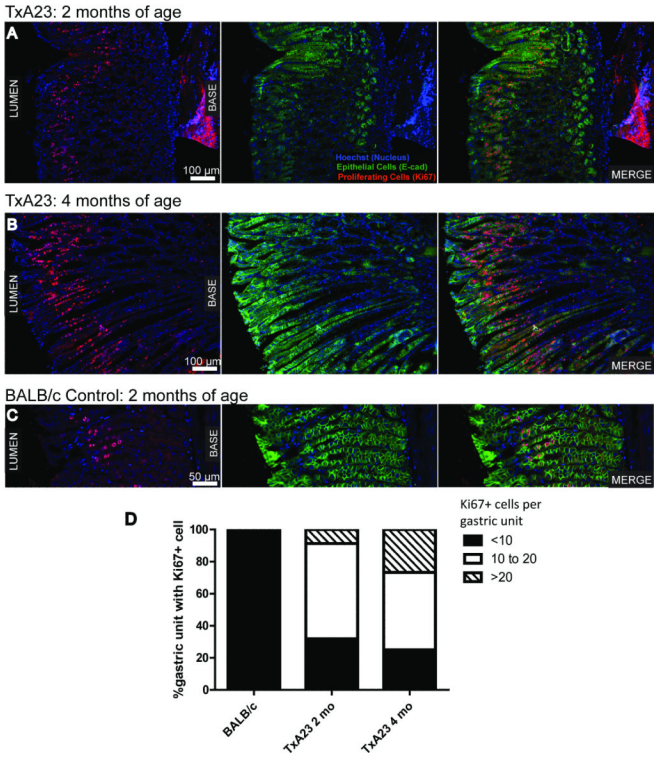

Figure 3. Increased epithelial cell proliferation in the gastric mucosa of TxA23 mice

(**A**-**C**) Images are representative of 2 month (**A**) and 4 month (**B**) old TxA23 mice and 4 month (**C**) old BALB/c stomach sections. E-Cadherin (green) stains epithelial cells, Ki67 (red) stains proliferating cells, and Hoechst (blue) was used to stain nuclei. (**D**) A quantitative analysis of the percent of gastric units containing proliferating epithelial cells (E-Cadherin^{+}Ki67^{+}) in BALB/c and 2 month and 4 month old TxA23 mice.

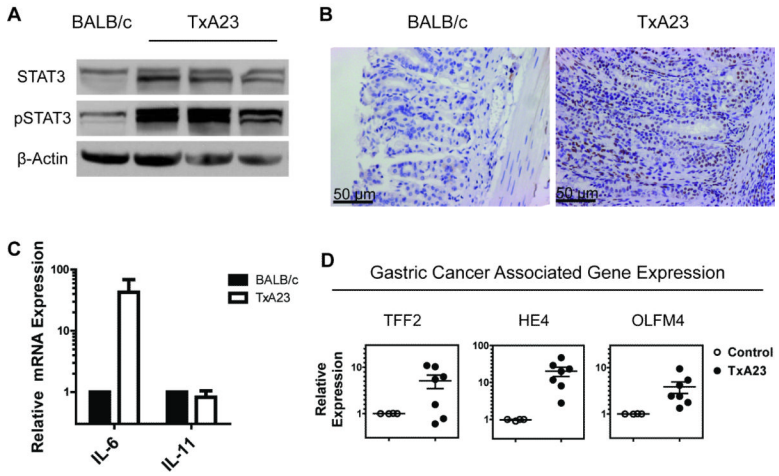

Figure 4. Increased levels of cancer associated markers in TxA23 mice

(**A**) Representative western blot of STAT3, pSTAT3 and β-Actin on whole stomach lysates of 2 month old TxA23 (n=9) and BALB/c mice. (**B**) Immunohistochemistry staining for pSTAT3 in gastric pits of BALB/c and TxA23 stomachs (magnified 20x). (**C**) The relative expression of IL-6 and IL-11 in mRNA extracted from the stomachs of TxA23 and BALB/c mice. (**D**) The relative expression of genes (HE4, TFF2, and OLFM4) that serves as biomarkers for the SPEM and preneoplastic progress was compared between mRNA isolated from the stomachs of TxA23 mice and BALB/c controls.

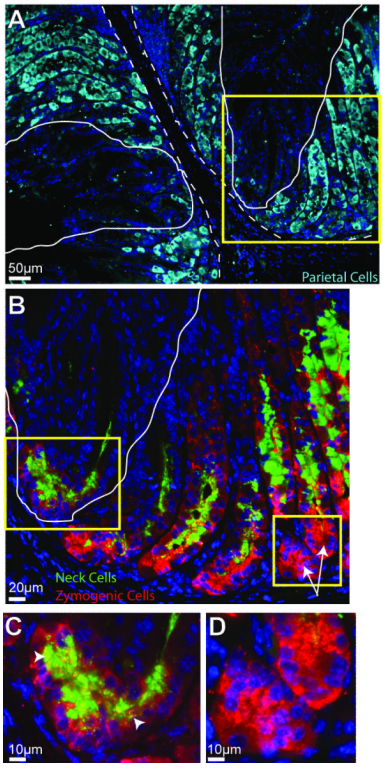

Figure 5. TxA23 mice have distinct regions of parietal cell loss coupled with the emergence SPEM

Representative immunostains of the corpus region of the stomach of TxA23 transgenic mice. (**A**) The lamina propria is separated from the glandular mucosa by the white dotted lines wherein parietal cells are stained with VEGFB (teal) and nuclei with Hoechst (blue). Note the distinct regions of parietal cell loss as highlighted by solid white lines. (**B**) The area highlighted by the yellow box in panel A has been stained with GSII (green, neck cells), GIF (red, ZC), and Hoechst (blue, nuclei). The yellow box on the left indicates a region of SPEM where cells co-express GSII and GIF (white arrowheads). This region of the stomach has shown considerable parietal cell destruction. (**C**) Higher magnification of this region is shown below. (**D**) White arrows indicate areas of relatively normal gastric epithelial cell differentiation which correlate with regions where parietal cell numbers are normal. Further magnification of this region is shown below.

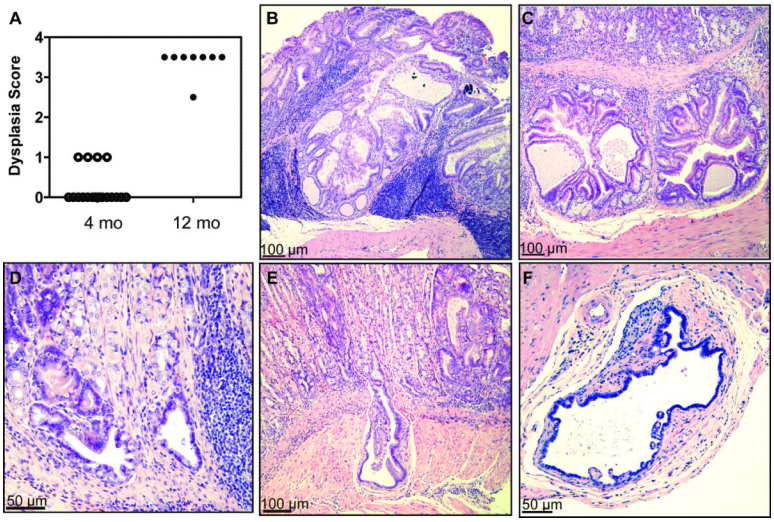

Figure 6. TxA23 mice develop masses with dysplastic foci as they age

(**A**) Dysplasia scores (where 1 = irregular glad forms, 3 = severe loss of glands and of columnar orientation of epithelium with regions of cellular atypia, increased mitotic figures, and 0.5 added when invasion of muscle or carcinoma in situ is identified) for sections at give ages. Each point represents an individual mouse. (**B**) Section of a mouse at 10 months of age (magnified 10×). Note to formation of mass with abundant, dense chronic inflammatory infiltrates. (**C-F**) Images of stomach sections that represent pathology observed in 12 month old mice with various degrees of pseudoinvasion of irregular glands into the submucosa. (**C**) Section showing submucosal focus of irregular gland formations (magnified 10×). (**D**) Section showing focus of irregular glands in submucosal tissue with surrounding chronic inflammation (magnified 20×). (**E**) Section showing deep submucosal pseudoinvasion by an irregular gland (magnified 10×). (**F**) Irregular glandular form on the adventitial surface of the stomach (magnified 20×).